X-ray Nano- and Micro-tomography in an SEM

Bart Pauwels* and Alexander Sasov
Bruker microCT, Kartuizersweg 3B, 2550 Kontich, Belgium
*Bart.Pauwels@bruker-microct.com

Introduction

X-ray microfocus computer tomography (μ-CT) is a non-destructive experimental technique that reveals the 3D internal microstructure of the sample under study [1]. The experimental set-up consists of an X-ray source, an X-ray detector, and set in between is a sample that is placed on a rotation stage. With this set-up multiple X-ray projection images can be obtained from the sample at different angles. In between the acquisition of two successive images, the sample is rotated over a small angle, typically between 0.2° and 1°. This set of projection images is then used as input for the reconstruction algorithm, which calculates a reconstruction of the internal microstructure of the sample with (sub-) micrometer sensitivity.

Scanning electron microscopy (SEM) on the other hand is used to study the topographic features and elemental composition of the surface of the sample [2]. The two techniques thus give different, complementary information about the sample. Until now, both techniques also required their own dedicated experimental set-up. This article describes new instrumentation for an SEM that adds micro- and nano-tomography capabilities to most commercial SEMs. Submicrometer isotropic spatial resolution in 3D reconstructed images can be produced without making any modifications to the SEM. This micro-CT add-on for SEM is commercially available from Bruker [3].

Methods And Materials

Working principle. Figure 1 shows the construction and working principle of the micro-CT apparatus for an SEM. The micro-CT attachment consists of two devices: the microscanner and the camera assembly. The microscanner sits on the specimen stage of the SEM. The two main parts of the microscanner are a metal target for the X-ray generation and a precision rotation stage. The X-ray camera is installed on the wall of the SEM specimen chamber and is separated from the vacuum by a 250 μm beryllium window.

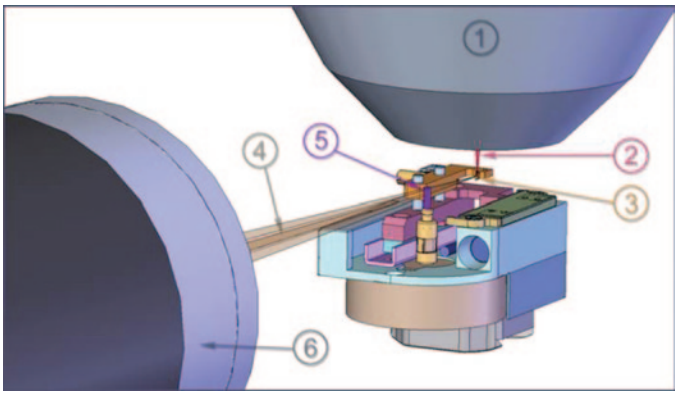

Figure 1: Set-up of the micro-CT unit on an SEM: (1) objective lens of the SEM, (2) electron beam, (3) metal target for X-ray generation, (4) X-ray cone beam, (5) sample positioned on the rotation stage, and (6) camera assembly.

The objective lens of the SEM focuses the electron beam onto the metal target positioned at the top of the microscanner. The metal target is inclined 45° with respect to the electron beam. Beam electrons excite the metal target atoms to produce X rays. To generate X rays at a small fixed location on the target, the SEM is switched to SPOT mode. Alternatively, if the SEM has no SPOT mode, image magnification is set to its maximum value. A portion of the generated X rays passes through the sample installed on the rotation stage. X-ray projection images of the sample are collected by the X-ray camera and digitized as 16-bit images. There are two options for the X-ray camera: either a front-illuminated 512 × 512 pixel charge coupled device (CCD) or a back-illuminated deep-depletion 1k × 1k CCD, each with single-photon detectability. The front-illuminated 512 × 512 CCD camera has 24 μm square pixels, and the 1k × 1k deep-depleted camera has 13 μm square pixels. Both cameras are cooled to reduce thermal electron noise. Multiple frames of the same image can be averaged to further reduce noise.

The geometrical magnification M in this setup is calculated as $M = R_2/R_1$ where R_2 is the distance from the X-ray emission point to the camera and R_1 is the distance from the X-ray emission point to the object. In this set-up, R_2 is fixed by the geometry of the SEM specimen chamber, while R_1 can be changed by a motorized stage on the microscanner. Typically image pixel sizes from 350 nm to 8 μm can be obtained.

Microscope settings and sample preparation. To keep the exposure time and the gain of the X-ray camera as low as possible, a high beam current is needed to create enough X-ray flux. The required e-beam current is at least 100 nA, often requiring the objective aperture to be removed from the beam path. The size of the focused electron beam on the metal target can be judged from the secondary electron (SE) or backscattered electron (BE) image of the target surface; sharp SEM images indicate good focusing to a small electron spot size. This results in a small X-ray generation area and consequently in sharp X-ray images. When scanning at small pixel sizes (below 800 nm), the largest objective lens aperture can be introduced into the electron beam path to produce a smaller X-ray spot size [4].

Preparation of samples for examination by micro-CT in the SEM is straightforward. A small piece of sample (diameter: 0.5–1 mm) is placed on a specimen holder and fixed with a small amount of wax or glue. In the SEM, scattered electrons may charge non-conductive samples. This will cause an unwanted movement of the X-ray spot because a charged sample surface can influence the position of the electron beam, resulting in blurring artifacts in the image reconstruction. There are two ways to prevent this charge accumulation: samples may be coated with a thin conductive layer, for example, Au-Pd, or, alternatively, a small conductive cap that is transparent to X rays can be placed over the sample.

X-ray spectrum and camera selection. Because most SEMs have an upper limit of electron acceleration voltage of 30 kV, the maximum energy of the emitted X-ray spectrum is limited to 30 keV. Figure 2a shows a simulation of the X-ray spectra generated

 doi:10.1017/S1551929513000047

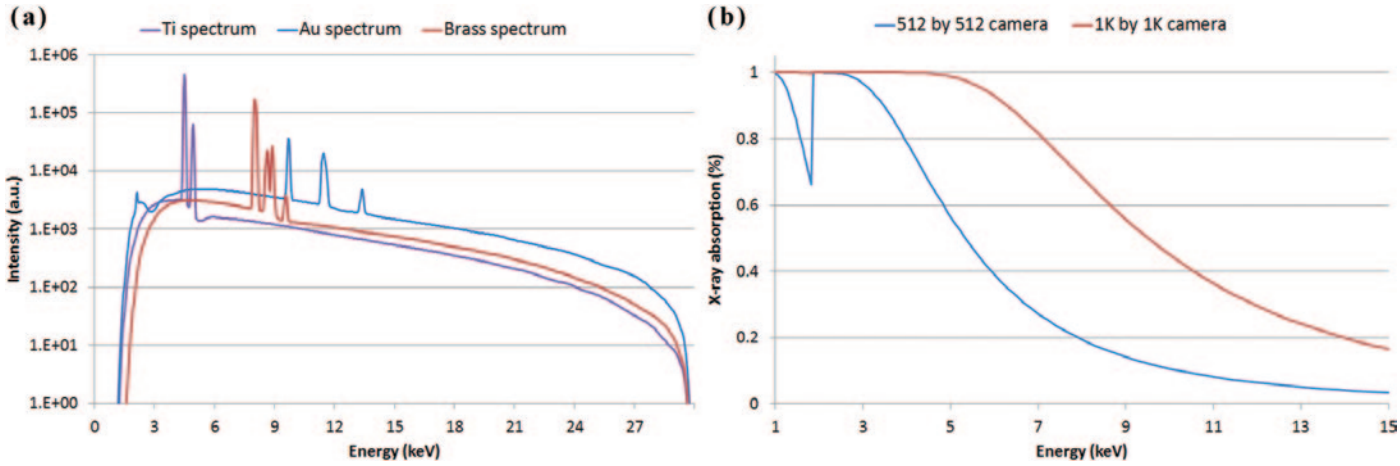

Figure 2: (a) Simulation of the X-ray spectra of a Ti, Au, and brass bulk target. The spectra are simulated with a 250 μm Be window in front of the detector. (b) Absorption curves for X rays in 15-micrometer detection layer of Si (front-illuminated 512 × 512 camera) or an 80-micrometer Si layer (deep-depleted 1k × 1k camera).

when 30 keV electrons hit bulk targets of different materials. These simulations were produced using Win X-ray [5]. The X-ray emission spectra exhibit strong characteristic peaks corresponding to the target material superimposed on a background of continuous radiation (Bremsstrahlung). Because the Bremsstrahlung background is low compared to the characteristic peaks, the X-ray spectrum can be considered as quasi mono-energetic with an average energy that is determined by the characteristic peaks. The characteristic X-ray energy can be easily tuned by changing the target material. In this way, the contrast of the X-ray projection images can be optimized for different samples.

It is important that the X-ray camera is sensitive to the emitted X-ray spectrum. The choice of target material, which determines the X-ray spectrum, has implications for the camera choice and vice versa. The 512 × 512 direct-detection camera has a detection layer of 15 μm of Si, whereas the deep-depleted camera has an active Si layer of 80 μm. Figure 2b shows absorption curves for X rays traveling through 15 μm and 80 μm of Si. These curves indicate the detection efficiency of the two cameras. For the 512 × 512 camera, the maximum of the absorption curve is between X-ray energies of 2 keV and 3 keV, and this curve drops rapidly at higher energies. For the deep-depleted camera, detection efficiency starts to decrease at 5.5 keV, and this drop-off is less rapid. At an X-ray energy of 8 keV (Cu K_α characteristic peak), the detection efficiency is 67% for the deep-depleted camera and 19% for the direct-detection camera. Because of the relatively low average X-ray energy, Si-based direct-detection X-ray cameras can be used for imaging. Low-density samples are imaged with the front-illuminated camera in combination with a Ti target, whereas the deep-depleted camera is more suited for denser samples in combination with a brass or Au target.

Resolution-determining factors. An important characteristic of a CT system is the spatial resolution. The two main limitations on the reconstructed image resolution are the X-ray spot size and the accuracy of the stage rotation. When 30 keV electrons impinge on a bulk target, the diameter of the X-ray generation volume, and consequently the emitted X-ray spot size, is expected to be in the micrometer range [2]. The X-ray spot size also depends on other parameters such as the type of metal target and the electron beam divergence angle, which is determined by the diameter of the objective lens aperture [4].

Results

Not all samples are suited to the SEM-based micro-CT device. Because the X-ray energy is limited, only low-density samples that are not too radiopaque can be scanned. Typical sample types are biological samples such as small insects, seeds, wood, small fossils, and materials such as foam structures, polymers/plastics, carbon-based materials, paper, and filters.

Damselfly. Figure 3 shows a CT scan of the back part of a damselfly made with the SEM-CT attachment installed on a JEOL JSM 7000F. This microscope has a Schottky field emission electron gun that can be operated up to an accelerating voltage of 30 kV and a beam current of 850 nA. A titanium target generated the X rays, so the most intense energy in the emitted spectrum was 4.5 keV (see Figure 2a). The images were made using the 512 × 512 direct-detection camera. Scanning parameters were the following: exposure time = 4 s, rotation step = 0.9°, and frame averaging = 2. The scan duration was 39 minutes. The sample was prepared by critical point drying to prevent cracking. The sample itself was approximately 1.5 mm in diameter and was imaged with a pixel size of 3.1 μm. With a physical camera pixel size of 24 μm, this corresponds to a magnification of 7.8 times (magnification = physical pixel size/object pixel size).

A standard filtered back projection (FDK) algorithm was used for reconstruction [6, 7]. Because projection images here are relatively noisy, they were pre-processed with a 2D Gaussian smoothing. During reconstruction, it is possible to correct for small misalignment and for artifacts such as rings and beam hardening [1]. Ring artifacts appear when the response of an individual pixel (or a cluster of pixels) deviates systematically from its neighbors. With the direct-detection camera, where all pixels have equal sensitivity [8], reconstructions are free of ring artifacts. The ring artifact correction is the only procedure that requires the presence of all angular projections before reconstruction. Because this procedure is not necessary here, the reconstruction can run during the acquisition cycle, and the reconstructed images can be viewed immediately after the scan is finished.

Figure 3a shows one X-ray projection image from a set of 203 projection images that was acquired. Figure 3b shows a single coronal reconstructed slice through the sample. While in all projection images thickness information is superimposed, this information can be retrieved after reconstruction. In the

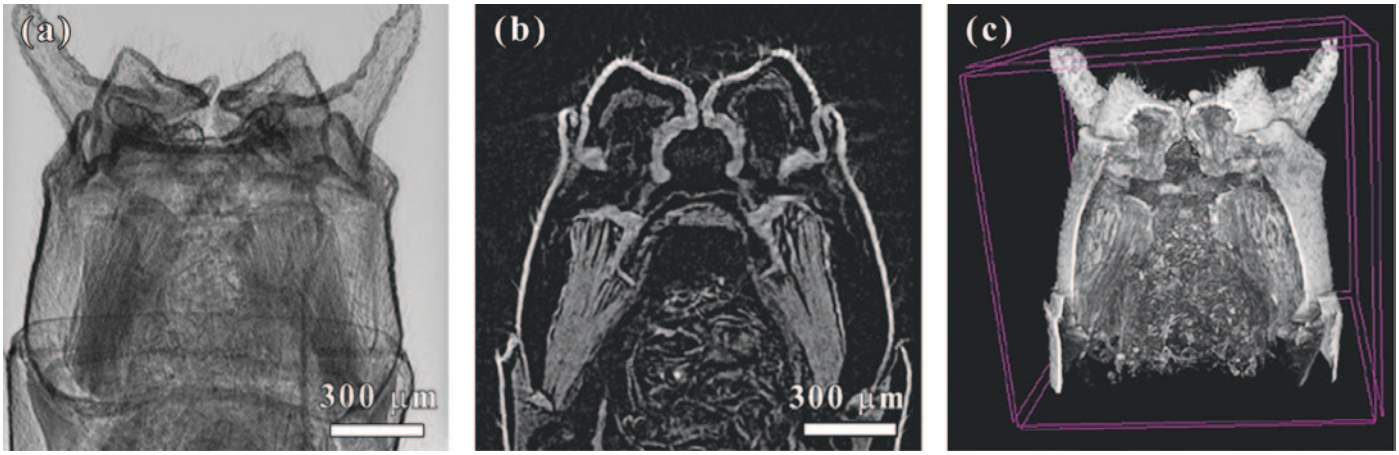

Figure 3: (a) One projection image of the abdomen of the *Ischnura Elegans*, (b) a reconstructed coronal slice showing clasper organs, and (c) a volume-rendered image based on the reconstructed slices. A wedged cut-out is made so the intestines and the clasper organs become visible.

section shown in Figure 3b, the clasper-organs at the tip of the abdomen and the intestines of the damselfly (*Ischnura Elegans*) can be observed. In order to have a 3D view of the sample, a volume-rendered image of the whole sample can be made (see Figure 3c). A virtual cut-out was made in the model to observe the interior of the damselfly.

Graphite. Figure 4 shows a CT scan of a porous carbon sample. This CT scan was made on the same SEM as the previous example: accelerating voltage was 30 kV and beam current was 850 nA. The deep-depleted 1k × 1k camera was used. The pixel size was set to 1.49 µm, corresponding to a magnification of 8.7. The field of view of the camera was 1.5 mm, whereas the diameter of the sample was 2 mm in size. Only the part of the sample within the field of view during the whole CT scan could be reconstructed. The exposure time per image was 6 s, and a frame averaging of 3 frames was used. The rotation step was 0.45°. Total scan time was 140 minutes. Figure 4 shows the porous structures of the graphite sample both in the reconstructed slices (Figure 4b) and in the volume-rendered image (Figure 4c).

Resolution of the system. The spatial resolution of the SEM-CT add-on was measured according to the ASTM E1695-95 standard [9]. Figure 5 shows the result of this test where the resolution of the SEM-CT add-on was calculated to be 700 nm. This test was done with an objective lens aperture of 110 µm diameter, a bulk brass target, and the 512 × 512 direct-detection camera.

To improve the spatial resolution of the SEM-CT, it is necessary to reduce the X-ray generation area within the metal target. By using thin layer targets (for example, 200 nm of Au), as described in [10] and [11], spatial resolution can be improved to 150–200 nm. Recently, special geometries like rods were used as targets to obtain X-ray source sizes of ~50 nm [11, 12].

Discussion

There exist three techniques to reveal the 3D internal microstructure of a sample in an SEM: a focused ion beam-SEM combination (FIB-SEM), serial block-face SEM, and SEM-CT. With a FIB-SEM, a focused ion beam removes a surface layer of the sample, and afterwards an SEM image of the sample's surface is made. This results in a stack of 2D SEM images that represent the 3D structure of the sample. This technique is mostly used in materials science and the semiconductor industry.

Different kinds of atoms have a different removal rate for the FIB. When a layer consists of atoms with a different removal rate, the resulting surface after treatment will no longer be flat. The SEM image that is made of the non-flat surface will be used as a flat 2D layer in the stack of images. In this case, it is never

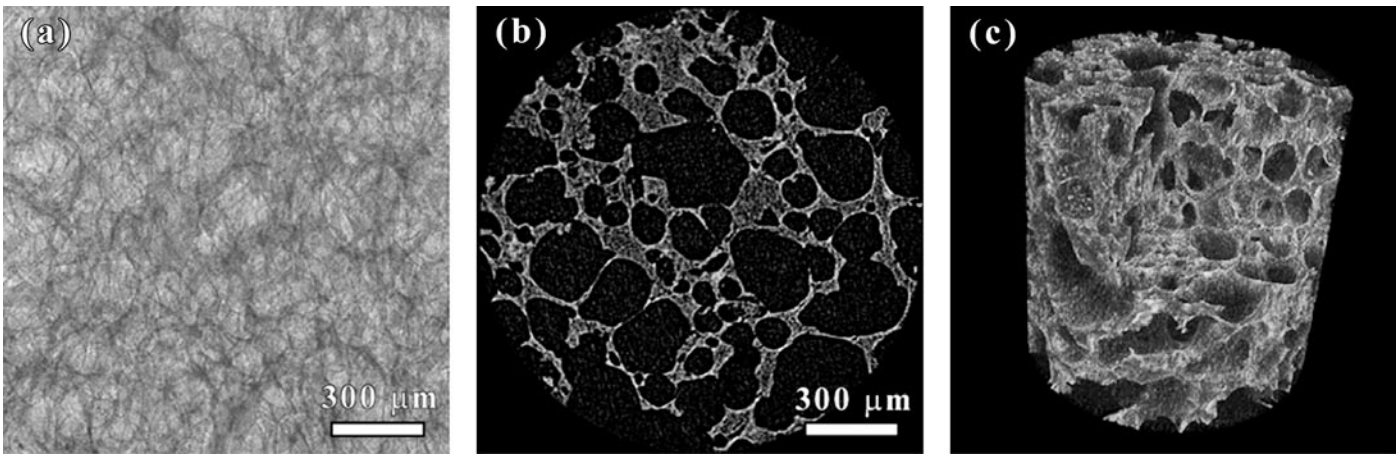

Figure 4: (a) Projection image of a graphite sample. The sample is larger than the field of view of the camera. (b) A reconstructed trans-axial slice where the pores can be easily measured, and (c) a volume-rendered image with a square cut-out.

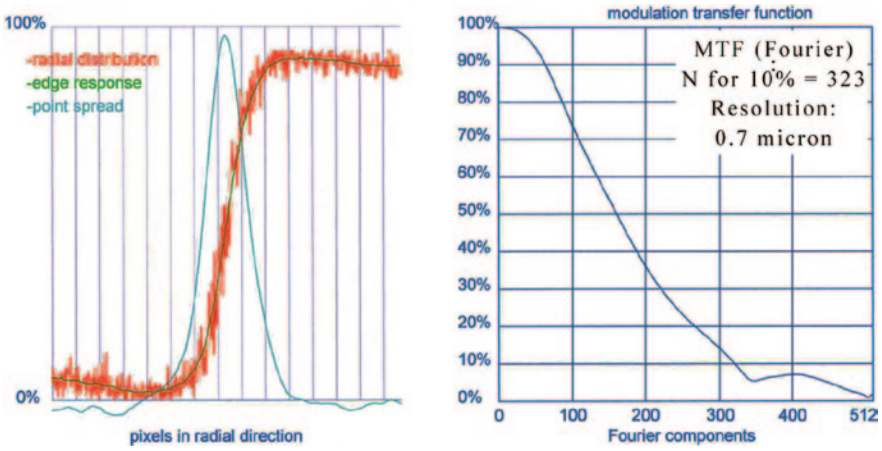

Figure 5: Results of the ASTM E1695-95 standard resolution test with the micro-CT unit installed on a JEOL JSM 7000F microscope (30 keV, 110 µm aperture, 290 nA). The edge of a transaxial slice of a cylindrical wire with radius R is used to calculate the edge response function and the point spread function. The x-axis of the left graph ranges from 0.9 × R to 1.1 × R. The modulation transfer function is the Fourier transform of the point spread function; the frequency with 10% modulation determines the resolution figure for the CT system.

certain that the imaged layers in the 3D stack really represent a flat cross section of the sample. In the case of SEM-CT, all virtual slices are ideally flat. The 3D structure of the sample is not distorted by sample preparation or imaging, and reliable 2D and 3D analysis of the internal micromorphology can be performed.

The serial block-face SEM is a combination of an SEM and an ultramicrotome mounted inside the specimen chamber of the SEM. The sample under study is embedded in resin. After each thin section is cut off by the microtome, the surface of the resin-embedded sample is imaged with the SEM. Again a stack of 2D SEM images is created that represent the 3D microstructure of the sample. This technique is mostly used to image biological specimens. In order to obtain good image contrast, most samples need to be stained. With SEM-CT, good contrast in the X-ray images can be obtained by changing the target material on the microscanner. Furthermore, sample preparation is much more demanding and time-consuming for serial block-face SEM compared to SEM-CT.

Both FIB-SEM and serial block-face SEM are destructive techniques, whereas SEM-CT is a non-destructive technique. The sample is still intact after acquiring all necessary images to reconstruct the 3D microstructure. This opens the possibility to scan the same sample repeatedly to evaluate microstructural changes due to, for example, loading, compression, or chemical modifications. The SEM-CT method is also less time-consuming. The scan time is independent of the magnification, whereas for the two destructive techniques the time to build the 3D stack depends on the required resolution in the direction perpendicular to the image plane.

The resolving power is different for the three techniques. The FIB-SEM can achieve the highest spatial resolution; it can remove layers with thicknesses around 5–10 nm, and the resolution within a 2D layer can be as small as 1–2 nm. The imaging resolution for the serial block-face SEM technique is the same, except that the resolution in *z*-direction is of the order of 30–50 nm. Both techniques can be used in combination with large samples. In SEM-CT, the pixel/voxel sizes are much larger, and the resolution is limited by the X-ray spot size (700 nm). With rod-shaped targets, there is the possibility to improve resolution to 50 nm (as described above). In SEM-CT, the voxels are isotropic, whereas for the other two techniques the voxels are anisotropic: the length in the *z* direction is different and larger than the length in the *x* and *y* direction.

Conclusions

This article describes an SEM-based micro-CT attachment that adds nano- and micro-tomography capabilities to almost any type of SEM. The microscanner, which holds the X-ray target and the rotation stage, is located on the specimen stage in place of the standard specimen mount, and the X-ray camera is fixed to a flange of the SEM specimen chamber. The camera used in the SEM-CT add-on is a CCD X-ray camera with single photon detectability. The uniform sensitivity of the detector eliminates ring artifacts. The overall resolution of the SEM-CT add-on is shown to be around 0.7 micrometers when using a brass X-ray target.

References

[1] SR Stock, *MicroComputed Tomography: Methodology and Applications*, Taylor & Francis, New York, 2008.

[2] J Goldstein, DE Newbury, DC Joy, P Echlin, CE Lyman, E Lifshin, E Sawyer, J Michael, *Scanning Electron Microscopy and X-ray Microanalysis*, Kluwer Academic/Plenum Publishers, New York, 2003.

[3] Bruker Corporation, "True 3D Microscopy for SEM," https://www.bruker.com/products/x-ray-diffraction-and-elemental-analysis/x-ray-microanalysis-and-ebsd/micro-ct-for-sem/overview.html.

[4] B Pauwels, X Liu, and A Sasov, "X-ray nanotomography in a SEM," *P Soc Photo-Opt Inst: Developments in X-Ray Tomography VII* 7804 (2010).

[5] R Gauvin, E Lifshin, H Demers, P Horny, and H Campbell, *Microsc Microanal* 12 (2006) 49–64.

[6] KA Feldkamp, LC Davis, and JW Kress, *J Opt Soc Am A* 1 (1984) 612–19.

[7] X Liu and A Sasov, "Cluster reconstruction strategies for microCT/nanoCT scanners," Proceedings of fully 3D image reconstruction meeting in radiology and nuclear medicine, July 6–9, 2005, Salt Lake City.

[8] Princeton Instruments, "Direct detection of x-rays (30eV to 20keV) using detectors based on CCD technology," http://www.princetoninstruments.com/Uploads/Princeton/Documents/TechNotes/Direct_detection_of%20_xrays_technote_1RevA0.pdf.

[9] ASTM E 1695-95 standard, "Standard test method for measurement of computed tomography (CT) system performance," 1995.

[10] P Bruyndonckx, A Sasov, and B Pauwels, *Powder Diffr* 25(2) (2010) 157–160.

[11] A Sasov, P Bruyndonckx, X Liu, and B Pauwels, *Imaging & Microscopy* 12 (2010) 18–20.

[12] A Sasov, B Pauwels, and P Bruyndonckx, "New type of lensless X-ray source for laboratory nano-CT with 50-nm resolution," *P Soc Photo-Opt Inst: Developments in X-Ray Tomography VII* 7804 (2010).

MT

- Cooling Stages
- Recirculating Heaters and Chillers
- Sputter Coaters
- SEM/TEM Carbon Coaters
- Vacuum Evaporators
- Glow Discharge Systems
- RF Plasma Etchers/ Plasma Reactors
- Critical Point Dryers
- Freeze Dryers
- Cryo-SEM Preparation Systems
- Vacuum Pumps & Accessories
- Evaporation Supplies
- **and more...**

well equipped...

Electron Microscopy Sciences is pleased to announce our new full line catalog, your comprehensive source for high-end Vacuum Equipment. EMS is committed to providing the highest quality products along with competitive pricing, prompt delivery and outstanding customer service.

and more...

Not just Vacuum Equipment, EMS also offers:

Laboratory Microwave Ovens • Automated Tissue Processors • Oscillating Tissue Slicers • Vibrating Microtomes • Rapid Immersion Freezers • Tissue Choppers • Desiccators and Desiccants • Centrifuges, Tubes, and Racks • Stirrers, Stirring Hotplates, and Digital Hotplates • Stirring Bars, Stirring Rods, and Hand Mixers • Vortex Mixers, Microplate Mixers, and Magnetic Stirrers • Tissue Rotators, Mixer Vortexes, and Rotator/Rockers • Dri Baths • Oven/Incubators • Cooling Chambers • Ultraviolet Lamps • Lab Jacks

For catalog requests, please visit our website at **www.emsdiasum.com**

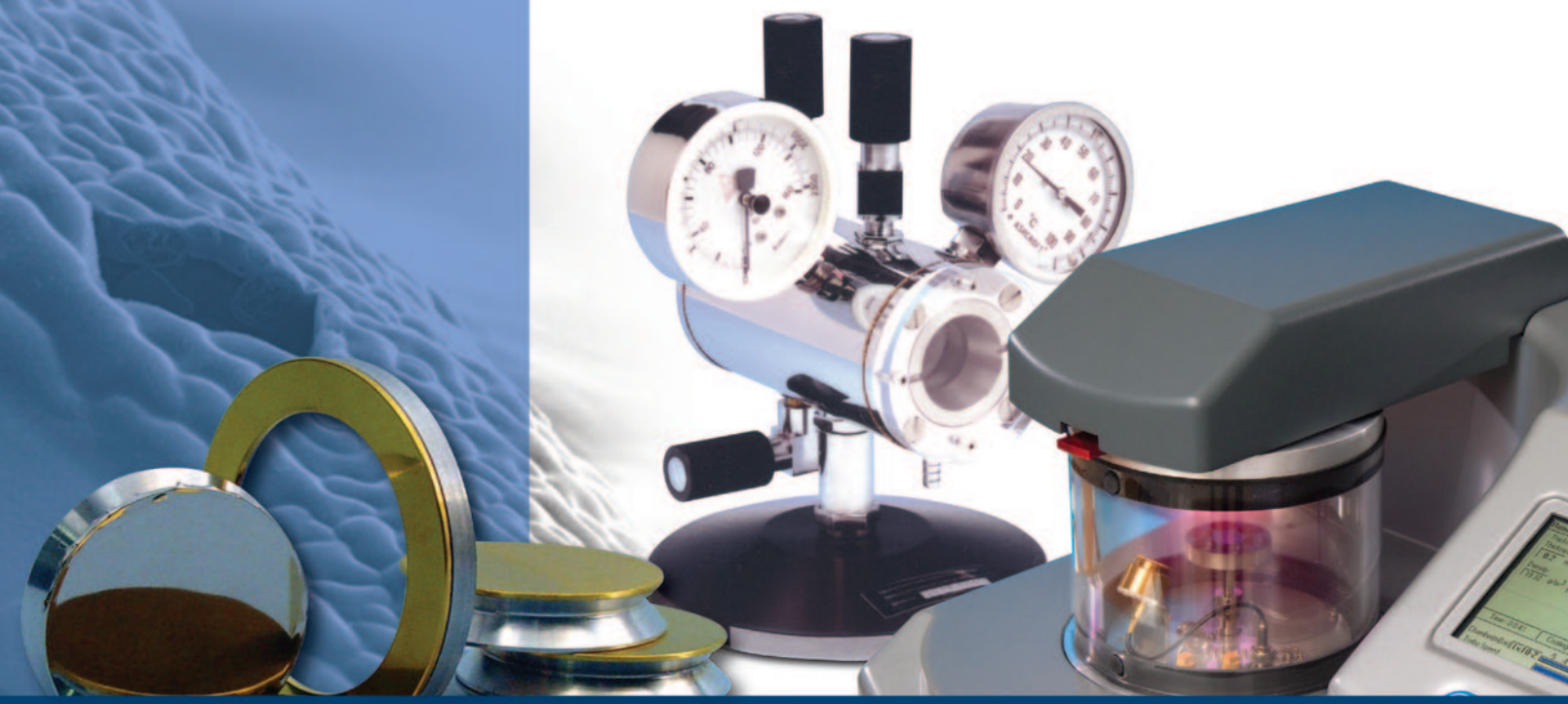

Electron Microscopy Sciences

Electron Microscopy Sciences
P.O. Box 550 • 1560 Industry Rd. • Hatfield, Pa 19440
Tel: (215) 412-8400 • Fax: (215) 412-8450
email: sgkcck@aol.com • www.emsdiasum.com